

Credit Counterparty Risk in the LGM Model

Financial Engineering Project

Original project co-authored with Alice Sofia Casciani. Final version
revised by Leonardo Bacchi for personal portfolio use.

Politecnico di Milano — MSc Mathematical Engineering —
Quantitative Finance

Academic Year: 2024–2025

Abstract

This work analyzes counterparty credit risk (CCR) for three portfolios of interest rate swaps using two one-factor short-rate models: Hull–White (HW) and Linear Gaussian Markov (LGM). Both models are calibrated to the same set of at-the-money swaptions.

In our implementation, the HW model jointly calibrates the mean reversion speed a and a single volatility level, while the LGM uses a piecewise-constant volatility structure, keeping a fixed from the outset.

Monte Carlo simulations were run over a 10-year horizon with different time grids: a quarterly grid to model collateral re-margining on a semi-annual basis, and weekly and daily grids to simulate collateral paid weekly. These simulations produce the main exposure profiles — expected exposure (EE), expected positive exposure (EPE), potential future exposure (PFE) and peak PFE — both with and without netting and collateral agreements.

Across all configurations, the two models show deviations below 5%, with a more noticeable difference only at the first time horizon.

The results indicate that, for standard swap portfolios and a relatively smooth volatility surface as observed in the available data, the greater structural flexibility of the LGM does not lead to significant differences in counterparty risk metrics. However, the more detailed parameterization does not result in higher calibration or simulation times: the additional burden is conceptual, not computational.

The LGM remains a more general extension of the HW model and may offer advantages in markets characterized by strong curve irregularities or in the valuation of optional or path-dependent instruments.

Table of Contents

1	Calibration of the Hull-White Model to Swaption Data	3
1.1	Theoretical Background	3
1.2	Bootstrap of the Discount Curve	3
1.3	Market Volatilities and Scaling Conventions	3
1.4	Pricing Diagonal Swaptions under Black and Bachelier	4
1.5	Jamshidian's Decomposition in the Hull-White Model	4
1.6	Numerical Calibration via Constrained Optimization	5
2	Formulation and Pricing of Swaptions in the Linear Gaussian Markov (LGM) Framework	6
2.1	Derivation of the Forward Stochastic Discount Factor under LGM Model	6
2.2	Swaption Pricing via Jamshidian's Decomposition	9
3	Piecewise-Constant Volatility Calibration of the LGM Model	10
3.1	Calibration via Jamshidian	10
3.1.1	Extended bond-put pricing formula	10
3.1.2	Bootstrap calibration algorithm	10
3.1.3	Results	11
4	Monte Carlo Simulations for Counterparty Credit Risk	12
4.1	Uncollateralized and Non-Netted Case	12
4.2	Netting and Collateral Case	14
4.2.1	Portfolio Alpha	14
4.2.2	Portfolio Beta	15
4.2.3	Portfolio Gamma	17
4.3	Model Comparison and Portfolio Insights	19
4.3.1	Comparison between LGM and Hull-White Models	19
4.3.2	Impact of Using Par versus Non-Par Swap Rates	19
4.4	Collateral Posting on a Weekly Basis	19
4.4.1	Collateral Posting with Weekly Time Grid	19
4.4.2	Collateral Posting with Daily Time Grid	20
4.5	Computational Challenges and Optimizations	20

1 Calibration of the Hull-White Model to Swap-tion Data

1.1 Theoretical Background

The Hull–White one-factor model assumes that the instantaneous short rate $r(t)$ follows a mean-reverting Ornstein–Uhlenbeck process under the risk-neutral measure:

$$dr(t) = [\theta(t) - ar(t)] dt + \sigma dW(t), \quad (1)$$

where:

- $a > 0$ is the mean-reversion rate, governing the speed with which $r(t)$ reverts to its long-term mean level.
- $\sigma > 0$ is the instantaneous volatility of the short rate.
- $\theta(t)$ is a deterministic function chosen so that the model exactly fits the initial term structure of interest rates.
- $W(t)$ is a standard Brownian motion under the risk-neutral measure.

The calibration task consists in choosing (a, σ) so that model-implied prices of a set of liquid instruments (in our case, European swaptions) most closely match their market quotes.

1.2 Bootstrap of the Discount Curve

Market quotes for deposit rates, futures and plain-vanilla swaps were used to construct a smooth zero-coupon curve. Although FRA rates were available in our Excel dataset, we chose to omit them from the interpolation. Starting from the shortest deposit maturities and advancing through futures and swap par-rates, we bootstrapped discount factors $B(0, t_i)$ for all tenors up to 50 years. This procedure provides a complete term-structure of discount factors—well beyond the range of our swaption expiries—and serves as deterministic input to all subsequent pricing formulas.

1.3 Market Volatilities and Scaling Conventions

For the swaption calibrations, the data provided did not clearly specify whether the market-implied volatilities referred to the Black or the Bachelier model. Although the latter seemed the more reasonable choice, we initially proceeded by considering both possibilities in parallel:

- **Black volatilities**, expressed in percent per annum. In our implementation they are rescaled in the Black-model pricing formula as $\frac{\sigma_{\text{Black}}}{100}$.
- **Bachelier volatilities**, quoted in basis points. Accordingly, before using them in the normal-model formula they are rescaled in the Bachelier-model pricing formula as $\frac{\sigma_{\text{Bach}}}{10000}$.

We focus on diagonal swaptions—i.e. options whose expiry and underlying swap tenor coincide—for expiries ranging from three months to ten years.

1.4 Pricing Diagonal Swaptions under Black and Bachelier

To measure the discrepancy between model and market, we first compute the market prices of each swaption. Concretely:

- under the **Black model**, the payer swaption price is given by

$$SP_{\alpha\omega} = B(T_0, T_\alpha) \text{BPV}_{\alpha\omega}(T_0) \left\{ S_{\alpha\omega}(T_0) N(d_1^s) - k N(d_2^s) \right\},$$

with

$$d_1^s = \frac{1}{\sigma_{\alpha\omega}\sqrt{T_\alpha}} \ln\left(\frac{S_{\alpha\omega}(T_0)}{k}\right) + \frac{1}{2} \sigma_{\alpha\omega} \sqrt{T_\alpha}, \quad d_2^s = d_1^s - \sigma_{\alpha\omega} \sqrt{T_\alpha}.$$

The parameters $\sigma_{\alpha\omega}$ denote the market-observed volatilities for the swaption expiring at T_α with underlying swap tenor ω . The quantity $S_{\alpha\omega}(T_0)$ is the forward par swap rate at the valuation date T_0 . In our calibration we set the strike k equal to $S_{\alpha\omega}(T_0)$, thereby restricting attention to at-the-money swaptions.

- under the **Bachelier model**, the swaption price is given by

$$SP_{\alpha\omega} = \text{BPV}_{\alpha\omega}(T_0) \left\{ (S_{\alpha\omega}(T_0) - k) \Phi(d^s) + \sigma_{\alpha\omega} \sqrt{T_\alpha} \varphi(d^s) \right\},$$

with

$$d^s = \frac{S_{\alpha\omega}(T_0) - k}{\sigma_{\alpha\omega} \sqrt{T_\alpha}}.$$

1.5 Jamshidian's Decomposition in the Hull–White Model

In the Hull–White framework, European swaption prices admit an analytic representation via Jamshidian's trick. The key idea is to express the swaption as a portfolio of put options on zero-coupon bonds:

$$\text{Swaption}(K) = \sum_{i=1}^N \alpha_i P_{\text{put}}(K_i; T_0, T_i). \quad (2)$$

where, α_i are the cash-flow weights and each strike K_i is a bond-specific level determined by solving for x^* such that the par-bond's value equals one. In practice, x^* is found by root-finding on the coupon-bond price equation.

Under Hull–White, each put on a zero-coupon bond has an explicit closed-form price as a function of (a, σ) . The price at time t of a European put option with strike K on a zero-coupon bond maturing at time S , with option expiry T ($S > T$), is given by

$$P_{\text{put}}(t, T, S, K) = B(t, S) \Phi(h) - K B(t, T) \Phi(h - \sigma_p),$$

where

$$\sigma_p = \sigma \sqrt{\frac{1 - e^{-2aT}}{2a}} \frac{1 - e^{-a(S-T)}}{a}, \quad h = \frac{1}{\sigma_p} \ln\left(\frac{B(t, S)}{B(t, T) K}\right) + \frac{\sigma_p}{2},$$

This decomposition allows us to compute the model-implied swaption price for any (a, σ) with no Monte Carlo, but rather by evaluating a collection of bond-option formulas.

1.6 Numerical Calibration via Constrained Optimization

To determine the optimal parameters (a, σ) , we define the sum of squared errors between model-implied and market-observed swaption prices as

$$\text{SSE}(a, \sigma) = \sum_{j=1}^M (P_{\text{model}}^{(j)}(a, \sigma) - P_{\text{mkt}}^{(j)})^2,$$

where $P_{\text{model}}^{(j)}$ and $P_{\text{mkt}}^{(j)}$ denote the j -th swaption price from the Hull–White–Jamshidian routine and the market under either the Black or Bachelier convention, respectively. We then solve the constrained nonlinear least-squares problem

$$(a^*, \sigma^*) = \arg \min_{a, \sigma \geq 0} \text{SSE}(a, \sigma),$$

using MATLAB’s `fmincon` with bounds $a \geq 0$ and $\sigma \geq 0$. Starting from an initial guess (a_0, σ_0) , the algorithm iterates until convergence, yielding the calibrated pair (a^*, σ^*) , which is then used in all subsequent analyses.

The calibration produces the following (a, σ) pairs for the Black model and the Bachelier model, respectively.

Table 1: Calibrated parameters for Black and Bachelier models

Model	a calibrated	σ calibrated
Black	7.1%	2.8%
Bachelier	9.8%	1.3%

2 Formulation and Pricing of Swaptions in the Linear Gaussian Markov (LGM) Framework

In this section we generalize the Hull–White one-factor model by allowing the volatility to vary deterministically over time, giving rise to the so-called LGM (Linear Gaussian Markov). We begin by specifying the SDE for the state variable x_t with time-dependent volatility $\sigma(t)$, and then derive the resulting affine formulas for zero-coupon bond prices. From these we obtain a closed-form expression for the forward discount factor. Finally, we demonstrate how Jamshidian’s decomposition carries over to this time-dependent setting, yielding analytic swaption prices without recourse to Monte Carlo simulation.

2.1 Derivation of the Forward Stochastic Discount Factor under LGM Model

We work in the risk-neutral measure \mathbb{Q} and specify the short rate as

$$r_t = \varphi_t + x_t, \quad x_0 = 0,$$

with the Ornstein–Uhlenbeck dynamics

$$dx_t = -a x_t dt + \sigma(t) dW_t \quad (3)$$

where $a > 0$ is the mean-reversion speed, W_t a \mathbb{Q} -Brownian motion, and $\sigma(t)$ an arbitrary deterministic function.

Solution of the state factor. Equation (3) describes an Ornstein–Uhlenbeck process whose solution, for $t \geq s$, is

$$x_t = e^{-a(t-s)} x_s + \int_s^t e^{-a(t-u)} \sigma(u) dW_u. \quad (4)$$

Integral of the short rate. Define the cumulative short rate over the interval $[s, T]$:

$$\int_s^T r_t dt = \int_s^T \varphi_t dt + \int_s^T x_t dt \quad (5)$$

Substituting (4) yield

$$\int_s^T \varphi_t dt + x_s e^{as} \int_s^T e^{-at} dt + \int_s^T \left(\int_s^t \sigma(u) e^{-a(t-u)} dW_u \right) dt \quad (6)$$

The deterministic term evaluates to

$$e^{as} \int_s^T e^{-at} dt = \int_s^T e^{-a(t-s)} dt = \frac{1 - e^{-a(T-s)}}{a} =: \beta(s, T). \quad (7)$$

By Tonelli’s theorem (stochastic Fubini) we may exchange the order of integration in the stochastic convolution term:

$$\int_s^T \sigma(u) \left(\int_u^T e^{-a(t-u)} dt \right) dW_u = \int_s^T \sigma(u) \frac{1 - e^{-a(T-u)}}{a} dW_u =: \int_s^T \hat{\sigma}(u, T) dW_u,$$

where we define the effective volatility kernel

$$\hat{\sigma}(u, T) := \sigma(u) \beta(u, T), \quad \beta(u, T) = \frac{1 - e^{-a(T-u)}}{a}.$$

Stochastic discount factor. The stochastic discount factor from s to T is defined as the exponential of the negative accumulated short rate:

$$D(s, T) = \exp\left(-\int_s^T r_t dt\right).$$

Using the decomposition $r_t = \varphi_t + x_t$ and the result of the previous subsection, we may rewrite $D(s, T)$ as

$$D(s, T) = \exp\left(-\int_s^T \varphi_t dt - x_s \beta(s, T) - \int_s^T \hat{\sigma}(u, T) dW_u\right),$$

where $\beta(s, T)$ is the mean-reversion factor in (7) and $\hat{\sigma}(u, T) = \sigma(u)\beta(u, T)$ is the effective volatility kernel.

Conditional expectation and bond price. Taking \mathcal{F}_s -expectation eliminates the stochastic integral (the latter is a centred Gaussian), producing the zero-coupon bond price

$$B(s, T) := \mathbb{E}_s[D(s, T)] = \exp\left(-\int_s^T \varphi_t dt - x_s \beta(s, T) + \frac{1}{2} \int_s^T \hat{\sigma}(u, T)^2 du\right). \quad (8)$$

The $+\frac{1}{2}$ term is the usual moment-generating adjustment for a Gaussian random variable.

Dividing $D(s, T)$ by its conditional mean isolates the purely stochastic component, yielding an exponential martingale:

$$\frac{D(s, T)}{B(s, T)} = \exp\left(-\int_s^T \hat{\sigma}(u, T) dW_u - \frac{1}{2} \int_s^T \hat{\sigma}(u, T)^2 du\right).$$

Forward stochastic discount factor. For any $s \leq T$ and tenor $\theta > 0$ define

$$B(s; T, T + \theta) := \frac{B(s, T + \theta)}{B(s, T)},$$

i.e. the price at time s of a unit payable at $T + \theta$ *per unit payable at T* .

Using the affine form of $B(s, T)$ in (8) one obtains

$$\begin{aligned} B(s; T, T + \theta) = & \exp\left(-\int_T^{T+\theta} \varphi_t dt - x_s [\beta(s, T + \theta) - \beta(s, T)]\right. \\ & \left. + \frac{1}{2} \int_s^{T+\theta} \hat{\sigma}(u, T + \theta)^2 du - \frac{1}{2} \int_s^T \hat{\sigma}(u, T)^2 du\right) \end{aligned} \quad (9)$$

At the reference date t_0 (typically today) the same forward price is deterministic:

$$B(t_0; T, T + \theta) = \exp\left(-\int_T^{T+\theta} \varphi_t dt + \frac{1}{2} \int_{t_0}^{T+\theta} \hat{\sigma}(u, T + \theta)^2 du - \frac{1}{2} \int_{t_0}^T \hat{\sigma}(u, T)^2 du\right). \quad (10)$$

Subtracting the deterministic exponent in (10) from (9) isolates the stochastic part and yields the compact representation

$$\boxed{B(s; T, T + \theta) = B(t_0; T, T + \theta) \exp\left(-x_s [\beta(s, T + \theta) - \beta(s, T)] - \frac{1}{2} \int_{t_0}^s [\hat{\sigma}(u, T + \theta)^2 - \hat{\sigma}(u, T)^2] du\right)} \quad (11)$$

where

$$\beta(s, T) = \frac{1 - e^{-a(T-s)}}{a}, \quad \hat{\sigma}(u, T) = \sigma(u) \beta(u, T).$$

Equation (11) shows that the forward bond price at time s is the initial forward price times an exponential adjustment that depends (i) *linearly* on the current state factor x_s and (ii) quadratically on the volatility kernel accumulated between t_0 and s . This decomposition is central to Jamshidian's approach, as it keeps the pay-off affine in x_s while capturing the time-dependent volatility structure of the LGM model.

2.2 Swaption Pricing via Jamshidian's Decomposition

As in the constant-volatility case, a European payer-swaption can be written as a sum of put options on zero coupon bond.

Forward stochastic discount. For any $T > T_\alpha \geq s$, the forward discount factor obtained in Section 2.1 reads¹

$$B(T_\alpha, T_\alpha, T) = B(t_0; T_\alpha, T) \exp\left(-x_s [\beta(T_\alpha, T) - \beta(T_\alpha, T_\alpha)] - \frac{1}{2} \int_{t_0}^T [\hat{\sigma}(u, T)^2 - \hat{\sigma}(u, T_\alpha)^2] du\right)$$

Fixed-leg coupon bond. Let the fixed leg of the underlying swap pay $C_i = \delta_i K$ at dates $T_{\alpha+1}, \dots, T_w$. The *coupon-bond* value at the option expiry T_α is

$$P_{cb}(T_\alpha) := \sum_{i=\alpha+1}^w C_i B(T_\alpha, T_i; X_{T_\alpha}),$$

where $B(T_\alpha, T_i; X_{T_\alpha})$ is the forward stochastic discount in the LGM model.

Swaption payoff. A payer-swaption with strike rate K is therefore a put on the above coupon bond with unit strike:

$$\text{Payoff}_{T_\alpha} = [P_{cb}(T_\alpha) - 1]^+.$$

Jamshidian root and individual strikes. Because every $B(T_\alpha, T_i; \cdot)$ is strictly decreasing in the sole state factor, there exists a unique x^* such that $P_{cb}(T_\alpha; x^*) = 1$. Define the bond strikes

$$k_i := B(T_\alpha, T_i; x^*), \quad i = \alpha + 1, \dots, w.$$

$$[P_{cb}(T_\alpha) - 1]^+ = \sum_{i=\alpha+1}^w C_i [B(T_\alpha, T_i; X_{T_\alpha}) - k_i]^+.$$

Present value at t_0 . Discounting by $D(t_0, T_\alpha)$ and taking expectations, the payer-swaption price becomes

$$\boxed{\text{Swpt}_{\alpha, w}(t_0) = \sum_{i=\alpha+1}^w C_i \mathbb{E}_{t_0} \left[D(t_0, T_\alpha) (B(T_\alpha, T_i; X_{T_\alpha}) - k_i)^+ \right]} \quad (12)$$

Interpretation. Equation (12) expresses the swaption as a sum of European puts on zero-coupon bonds with maturity T_i and individual strikes k_i . Closed-form formulas for each ZCB-put under the LGM dynamics are derived in Section 3.1 inserting them into (12) yields an analytic swaption price without Monte-Carlo simulation.

¹ $\hat{\sigma}(u, T) := \sigma(u) \beta(u, T)$ with $\beta(t, T) = \frac{1 - e^{-a(T-t)}}{a}$.

3 Piecewise-Constant Volatility Calibration of the LGM Model

3.1 Calibration via Jamshidian

In this section we describe how the LGM model is calibrated to the market swaption grid by exploiting Jamshidian's decomposition. The key idea is to extend the standard Hull–White bond-put formula so that it remains valid when the instantaneous volatility $\sigma(t)$ is deterministic but piece-wise constant. Once the closed-form expression is available, the calibration can be carried out swaption-by-swaption in a bootstrap fashion, which is far quicker than a simultaneous multi-parameter optimisation.

3.1.1 Extended bond-put pricing formula

For a European put exercisable at T on a zero-coupon bond maturing at $S > T$ the LGM price keeps the usual Black-type structure:

$$P(t_0, T, S) = K B(t_0, T) \Phi(-d_2) - B(t_0, S) \Phi(-d_1),$$

where

$$d_2 = \frac{\ln\left(\frac{B(t_0, S)}{K B(t_0, T)}\right) - \frac{1}{2} \Sigma^2}{\Sigma}, \quad d_1 = d_2 + \Sigma,$$

and $\Phi(\cdot)$ denotes the standard normal cumulative distribution function, while Σ^2 is the variance term appropriate to the LGM model. The cumulative variance term is defined as

$$\Sigma^2 = \int_{t_0}^T \sigma^2(r) [\beta(r, S) - \beta(r, T)]^2 dr,$$

With piece-wise constant volatilities σ_i on the intervals $[t_{i-1}, t_i]$ (the break-points are chosen to coincide with the swaption expiries), the variance splits into a finite sum:

$$\Sigma^2 = \sum_{i=0}^{j-1} \int_{t_i}^{t_{i+1}} \sigma_i^2 [\beta(r, S) - \beta(r, T)]^2 dr.$$

3.1.2 Bootstrap calibration algorithm

The summation formula above reveals an important monotonicity property: to price the swaption expiring at t_j only the first j volatilities $\sigma_1, \dots, \sigma_j$ are required independently of the swap tenor. This fact permits a sequential, or bootstrap, calibration:

- **First swaption** ($j = 1$). On the interval $[t_0, t_1]$ the model collapses to a constant-volatility Hull–White. We therefore recover σ_1 with the same root-finding routine employed in Section 1.
- **Subsequent swaptions** ($j = 2, \dots, n$). Assuming $\sigma_1, \dots, \sigma_{j-1}$ are already known, we determine σ_j by minimising the squared error between the market price and Jamshidian model price that embeds all previously calibrated

volatilities. The optimisation concerns a single scalar parameter and typically converges in a few iterations (tolerance $< 10^{-8}$).

3.1.3 Results

Calibration was performed on the diagonal ATM payer swaptions using both Black and Bachelier conventions. Table 2 reports the piece-wise constant volatilities σ_j obtained with Jamshidian’s bootstrap. Figure 1 plots the same values together with the constant Hull–White volatility from Section (1.6).

Table 2: Calibrated LGM volatilities σ_j (%)

j	1	2	3	4	5	6	7	8	9	10	11
Black	2.62	3.73	3.30	3.06	2.97	2.90	2.78	2.86	2.88	2.76	3.73
Bachelier	1.98	1.08	1.44	1.34	1.34	1.33	1.23	1.28	1.29	1.22	1.49

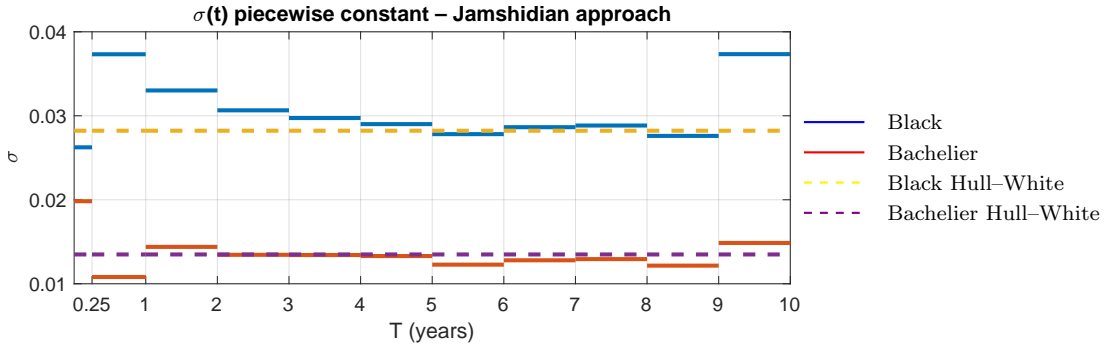


Figure 1: Piece-wise LGM volatilities calibrated with Black and Bachelier; the dashed line is the constant Hull–White volatility.

Model choice. Considering the implied volatilities quoted in basis points is much more natural, and with this interpretation their order of magnitude is compatible with the Bachelier model. For this reason, all subsequent sections refer to the calibration under the Bachelier framework shown in Table 2.

4 Monte Carlo Simulations for Counterparty Credit Risk

We now proceed to compute standard counterparty credit risk (CCR) measures—namely Expected Exposure (EE), Expected Positive Exposure (EPE), Potential Future Exposure (PFE), and peak PFE—under two different interest rate models: the Hull-White (HW) model and the Linear Gaussian Markov (LGM) model.

The HW model is calibrated as described in Section 1, using market data to estimate the parameters (a, σ) . For the LGM model, we use a fixed $a = 0.1$, a reasonable value and very close to the one found in the calibration of the Hull-White model, and calibrate eleven piecewise constant volatilities $\sigma(t)$ as described in Section 3.1. We perform the analysis for three different IRS portfolios (Alpha, Beta, Gamma) and under two distinct risk mitigation settings: one without collateral and netting, and another with both collateral and netting effects included.

Collateral is modelled as a process that resets the mark-to-market (MtM) to zero at each remargining date, effectively removing exposure on those dates. The collateral amounts are remunerated at the stochastic interest rate simulated according to the corresponding HW or LGM model. Netting is implemented by aggregating the MtM of all contracts facing the same counterparty into a single netted position. We repeat the entire analysis using three time-step granularities—quarterly, weekly, and daily.

4.1 Uncollateralized and Non-Netted Case

In this analysis, we computed the Mark-to-Market (MtM) values for each individual instrument within the portfolio. Subsequently, risk measures were calculated independently for each MtM value. Due to the nature of the uncollateralized and non-netted scenario, these individual risk measures were summed directly. Effectively, these risk measures represent counterparty risk; since netting is not permitted, aggregating MtMs by counterparty and subsequently calculating the risk measures was not possible. This scenario, therefore, implicitly treats each financial instrument as having its own distinct counterparty. This approach increases the overall counterparty risk measure, reflecting the absence of netting benefits in the risk exposure evaluation.

We present below the calculated risk measures for each of the three portfolios under analysis.

Table 3: Risk Measures without Collateral (in EUR millions)

Model	Alpha	Beta	Gamma
Peak PFE			
LGM	411.58	411.58	409.52
Hull-White	389.54	389.54	387.61
EPE			
LGM	84.51	84.51	84.14
Hull-White	81.61	81.61	81.27

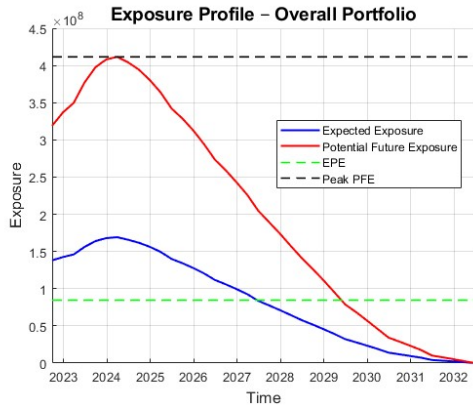


Figure 2: Exposure profile Portfolio Alpha under the LGM model.

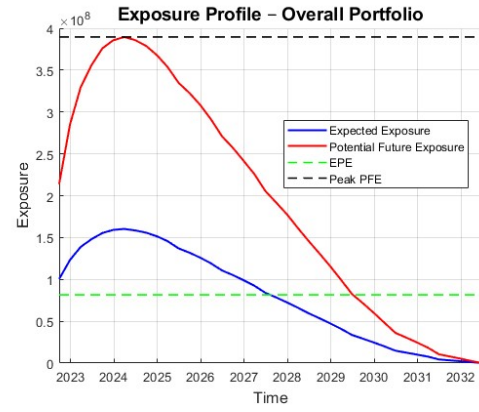


Figure 3: Exposure profile Portfolio Alpha under the HW model.

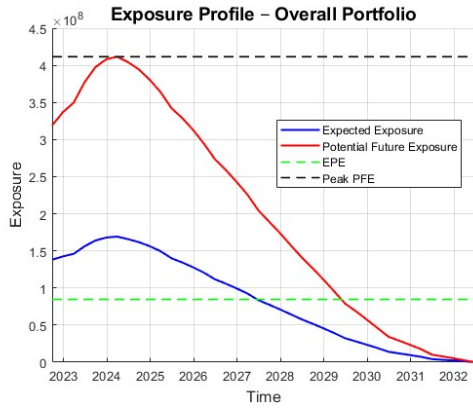


Figure 4: Exposure profile Portfolio Beta under the LGM model.

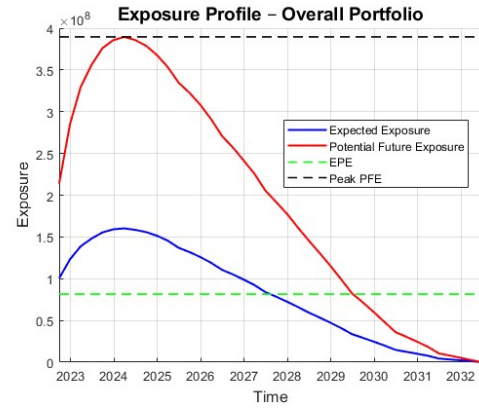


Figure 5: Exposure profile Portfolio Beta under the HW model.

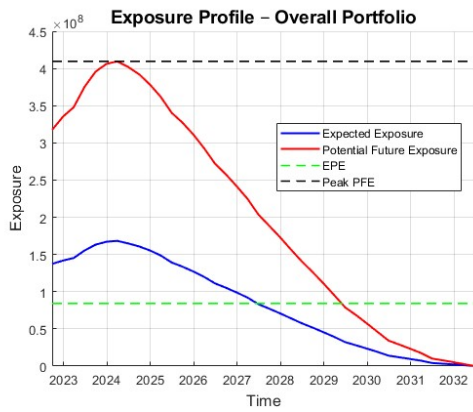


Figure 6: Exposure profile Portfolio Gamma under the LGM model.

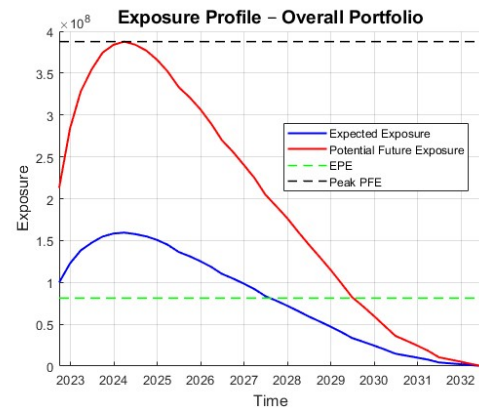


Figure 7: Exposure profile Portfolio Gamma under the HW model.

4.2 Netting and Collateral Case

In this section, we report the results of the counterparty credit risk analysis under the configuration with both netting and semiannual collateral remargining. The analysis is carried out separately for the two interest rate models considered: Hull–White and LGM. The relevant CCR metrics (EE, EPE, PFE, peak PFE) are computed using Monte Carlo simulations with 250000 scenarios.

4.2.1 Portfolio Alpha

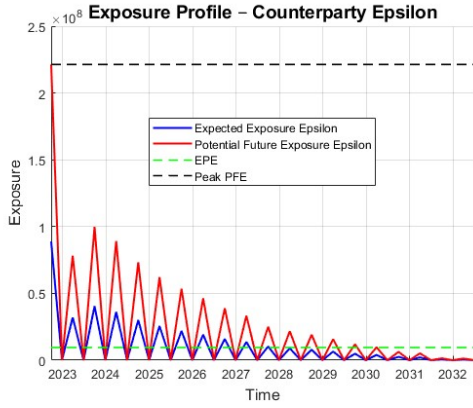


Figure 8: Exposure profile for counterparty Epsilon under LGM.

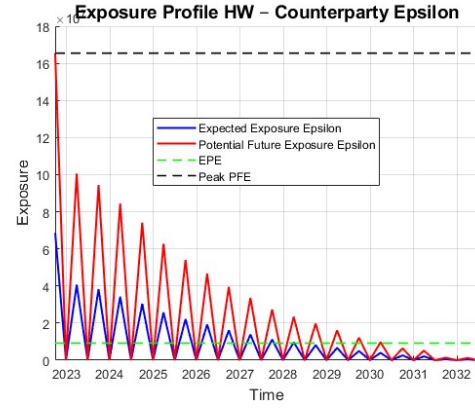


Figure 9: Exposure profile for counterparty Epsilon under HW.

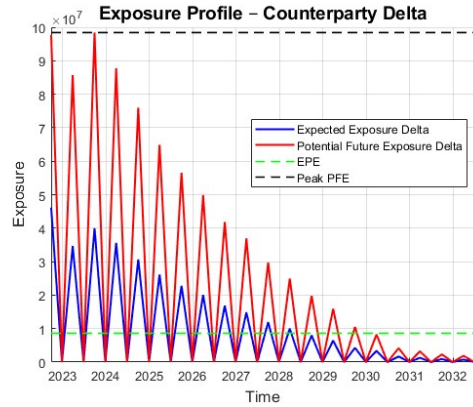


Figure 10: Exposure profile for counterparty Delta under LGM.

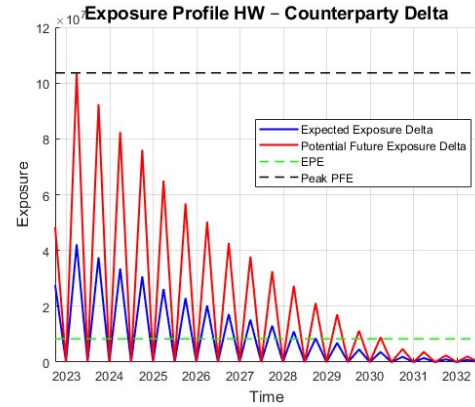


Figure 11: Exposure profile for counterparty Delta under HW.

We also computed the overall portfolio exposure by summing the risk measures of the two counterparties. The combined profiles under both models are shown in Figure 14.

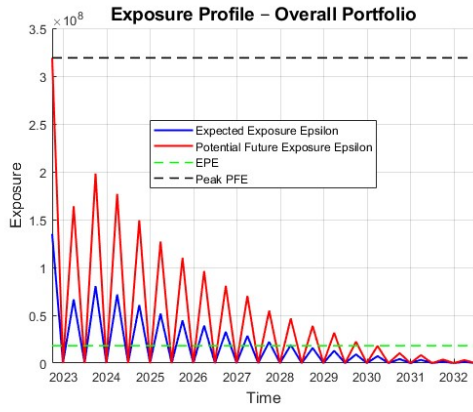


Figure 12: Exposure profile under the LGM model.

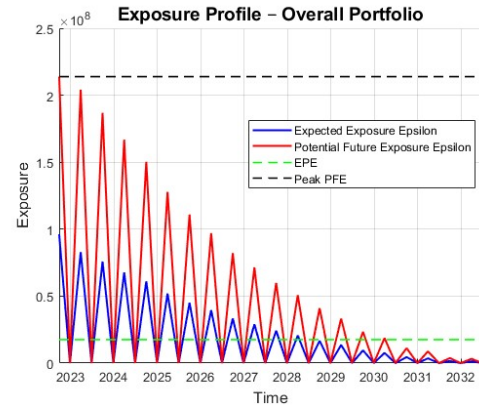


Figure 13: Exposure profile under the HW model.

Figure 14: Overall exposure for Portfolio Alpha.

4.2.2 Portfolio Beta

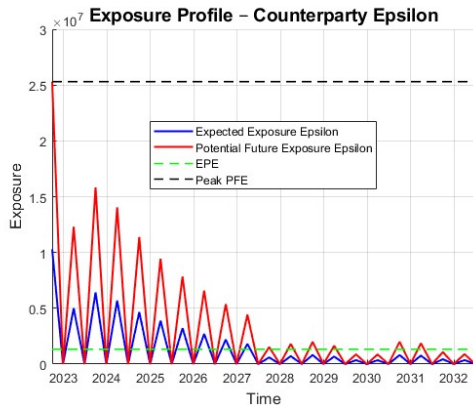


Figure 15: Exposure profile for counterparty Epsilon under LGM.

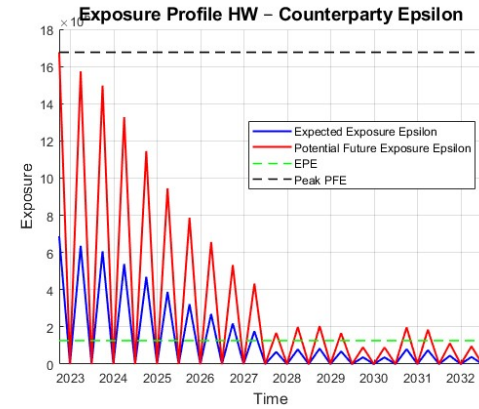


Figure 16: Exposure profile for counterparty Epsilon under HW.

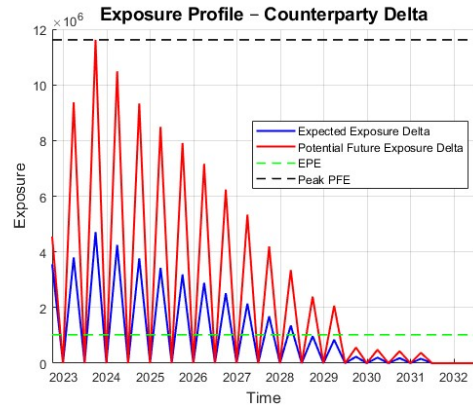


Figure 17: Exposure profile for counterparty Delta under LGM.

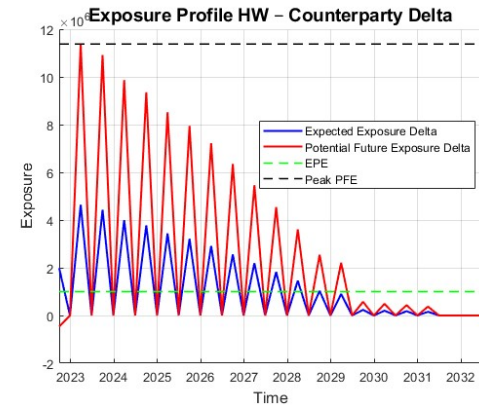


Figure 18: Exposure profile for counterparty Delta under HW.

We also computed the overall portfolio exposure by summing the risk measures of the two counterparties. The combined profiles under both models are shown in Figure 21.

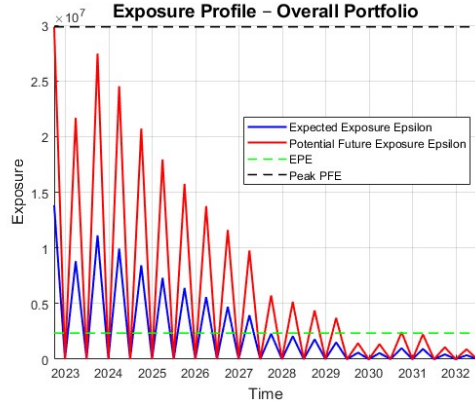


Figure 19: Exposure profile under the LGM model.

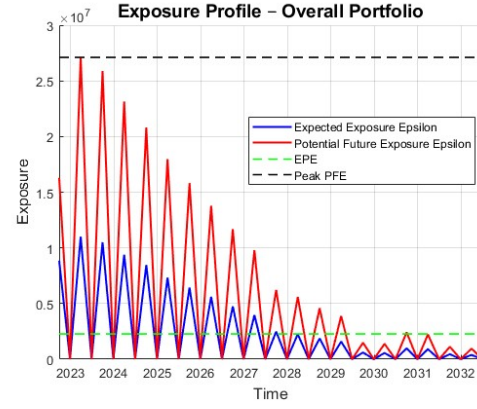


Figure 20: Exposure profile under the HW model.

Figure 21: Overall exposure for Portfolio Beta.

4.2.3 Portfolio Gamma

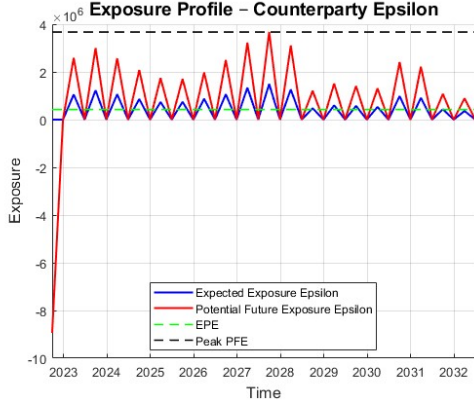


Figure 22: Exposure profile for counterparty Epsilon under LGM.

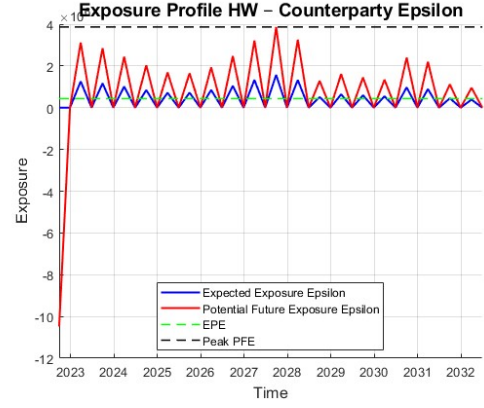


Figure 23: Exposure profile for counterparty Epsilon under HW.

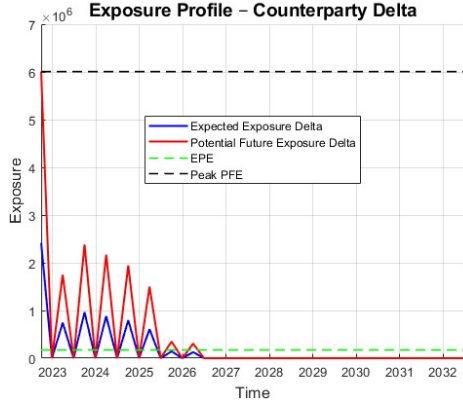


Figure 24: Exposure profile for counterparty Delta under LGM.

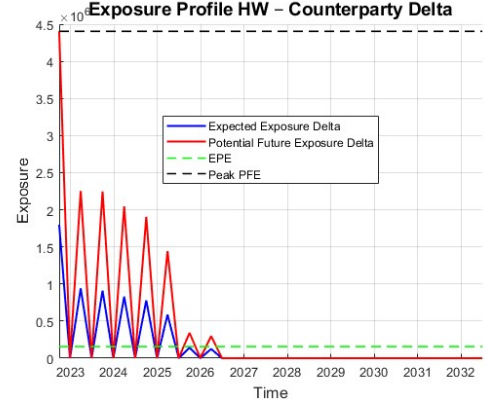


Figure 25: Exposure profile for counterparty Delta under HW.

We also computed the overall portfolio exposure by summing the risk measures of the two counterparties. The combined profiles under both models are shown in Figure 28.

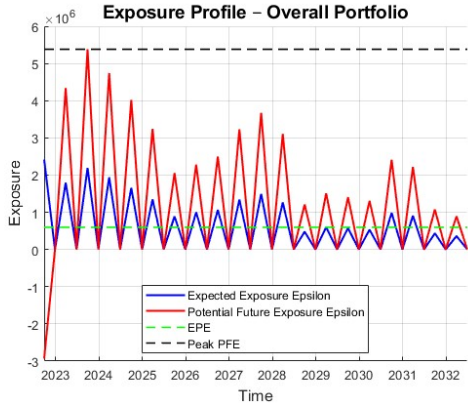


Figure 26: Exposure profile under the LGM model.

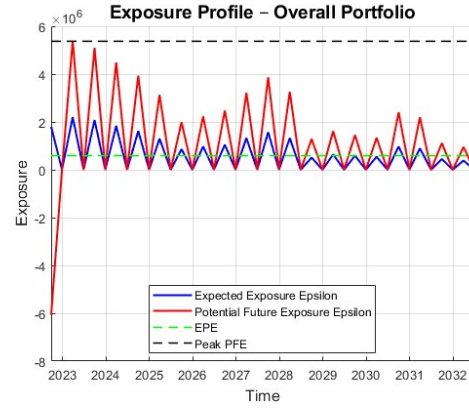


Figure 27: Exposure profile under the HW model.

Figure 28: Overall exposure for Portfolio Gamma.

To better understand the characteristics of the two counterparties, we first computed the risk measures separately by counterparty. The results are shown in Tables 4 and 5.

Table 4: EPE and peak-PFE under the LGM model (in EUR millions)

Portfolio	EPE Delta	peak-PFE Delta	EPE Epsilon	peak-PFE Epsilon
Alpha	8.62	98.42	9.52	221.35
Beta	1.02	11.62	1.33	25.30
Gamma	0.17	6.01	0.43	3.67

Table 5: EPE and peak-PFE under the Hull–White model (in EUR millions)

Portfolio	EPE Delta	peak-PFE Delta	EPE Epsilon	peak-PFE Epsilon
Alpha	8.36	103.65	9.21	165.46
Beta	1.00	11.38	1.26	16.77
Gamma	0.16	4.40	0.43	3.87

To evaluate the overall portfolio exposure, we sum the risk measures of the two counterparties. The aggregated results are presented in Tables 6 and 7.

Table 6: Total EPE and peak-PFE under the LGM model (in EUR millions)

Portfolio	EPE Total	peak-PFE Total
Alpha	18.143	319.030
Beta	2.348	29.851
Gamma	0.596	5.382

Table 7: Total EPE and peak-PFE under the Hull–White model (in EUR millions)

Portfolio	EPE Total	peak-PFE Total
Alpha	17.569	213.860
Beta	2.264	27.111
Gamma	0.588	5.373

4.3 Model Comparison and Portfolio Insights

4.3.1 Comparison between LGM and Hull–White Models

Across all three portfolios, the risk measures produced by the LGM and Hull–White models differ by less than 5% at nearly every grid point. The only exception is the three-month horizon, where the discrepancy is more pronounced. This is primarily due to the LGM calibration of the short-term instantaneous volatility $\sigma(t)$, which effectively mirrors the Hull–White behavior over such a limited time span. These results suggest that, within the context of this project, the additional theoretical complexity of the LGM model does not yield a significant improvement in the simulation outcomes compared to the Hull–White framework. In particular, the LGM model requires the mean reversion parameter a to be fixed a priori, with no straightforward way to calibrate it from market data. This limitation can be partially mitigated by adopting the value obtained from the Hull–White calibration.

Nonetheless, the LGM model represents a more general and theoretically accurate extension of the Hull–White model. Importantly, its increased complexity does not translate into higher computational costs—neither in calibration nor in simulation. The additional burden lies primarily in the model formulation and implementation, rather than in runtime performance.

It is also worth noting that the similarity observed in this study may not generalize to different market conditions or portfolio structures. The potential advantages of the LGM model could become more evident in contexts where market volatilities or structures deviate from the relatively regular patterns observed in our dataset.

4.3.2 Impact of Using Par versus Non-Par Swap Rates

For completeness, we repeated the entire CCR analysis using par-swap rates, rather than the “off-par” swap rates supplied in the assignment. The original, supplied rates tended to lie slightly above par. When we re-ran the simulations with true par rates, the initial peaks smoothed out and the profiles aligned more closely with theoretical expectations.

4.4 Collateral Posting on a Weekly Basis

4.4.1 Collateral Posting with Weekly Time Grid

With a weekly grid and weekly collateral, every margin call resets the mark-to-market to zero. Consequently, the entire MtM matrix becomes zeros for all counterparties, making EE, EPE, PFE, and peak-PFE trivially zero. We still imple-

mented and validated the routine—printing collateral flows for audit—and reduced the Monte Carlo scenarios to 2500 for reasonable turnaround.

4.4.2 Collateral Posting with Daily Time Grid

We also tested a daily grid while retaining weekly collateral dates. In this setting, only six of seven MtM rows between margin calls are non-zero; nevertheless, runtime grows sharply because A_t and C_t must be updated every step. For demonstration, we lowered scenarios to 100. The exposure profiles and collateral schedules are in the code notebook.

Table 8: EPE and peak-PFE under the LGM model (EUR millions), daily grid

Portfolio	EPE Delta	peak-PFE Delta	EPE Epsilon	peak-PFE Epsilon
Alpha	23.707	170.83	39.414	333.09
Beta	2.445	17.42	3.922	43.44
Gamma	0.419	6.92	0.389	4.28

Table 9: EPE and peak-PFE under the HW model (EUR millions), daily grid

Portfolio	EPE Delta	peak-PFE Delta	EPE Epsilon	peak-PFE Epsilon
Alpha	23.994	162.10	38.387	328.17
Beta	2.479	17.61	3.746	42.57
Gamma	0.393	6.82	0.399	4.68

4.5 Computational Challenges and Optimizations

Computing CCR metrics for large IRS portfolios—especially repeating the analysis for different configurations—proved non-trivial:

- **MtM valuation bottleneck.** Generating mark-to-market values for every swap in all three portfolios on a quarterly grid with 250000 Monte Carlo paths required approximately 100 s.
- **Scaling to finer time steps.** A denser grid forces recomputing the affine parameters A and C at each time step via our `affine_trick` routine, which is very sensitive to grid length and would substantially increase runtimes. Since the grid is uniform, we instead update (A, C) by dropping the last element and prepending zero. This shortcut introduces errors below 1% (mainly from date conventions) but drastically reduces computation time. For the quarterly, 250000-path runs the benefit was negligible, so for points (a) and (b) we retained the exact method.
- **Other optimizations considered.** Although some integrals could be computed in closed form, we opted to use the `quadgk` numerical integration routine for simplicity and generality. Caching invariant quantities (e.g. x_t and

stochastic discount factors) was also considered, but the potential speed-up was marginal and not worth the added complexity.

- **Parallelization attempt.** We experimented with MATLAB's `parfor` to compute each instrument's MtM in parallel, but observed no meaningful speed-up, and thus reverted to the serial implementation.

References

- [1] Brigo, Damiano, and Fabio Mercurio. *Interest Rate Models: Theory and Practice*. Vol. 2. Berlin: Springer, 2001.
- [2] Hagan, Patrick S. *Evaluating and Hedging Exotic Swap Instruments via LGM*. Bloomberg Technical Report, 2015.
- [3] Gregory, Jon. *Counterparty Credit Risk: The New Challenge for Global Financial Markets*. The Wiley Finance Series, 2010.